Proceedings of the
47th IEEE Conference on Decision and Control
Cancun, Mexico, Dec. 9-11, 2008

A Model Predictive Control Framework for Industrial Turbodiesel Engine Control

Gregory Stewart and Francesco Borrelli

Abstract— **This article describes the development and implementation of a practical explicit model predictive control (MPC) approach that allows subcontrollers to receive and accommodate time-varying setpoints and constraints from higher levels in standard industrial automotive controller hierarchies. The MPC approach requires a small computational footprint that is suitable for implementation within a modern electronic control unit (ECU). This article presents the approach, method of implementation, and preliminary results on a 2.2 litre turbodiesel engine.**

I. Introduction

The development of diesel engines requires the engine maker to achieve a successful tradeoff between fuel economy, drivability, and engine cost while respecting the constraints imposed by emissions legislation. As legislated emissions constraints are tightened, diesel engine makers are being required to increase the number of components in an engine - including sensors, actuators, and new subsystems such as diesel particulate filters (DPF) and selective catalytic reduction (SCR) [19]. At the same time the higher levels of performance require increased component reliability and consideration of the interactions between subsystems. This situation has ramifications in both the development of hardware components and the software implementation of control schemes that can deliver the required performance.

The automotive industry uses a wide array of approaches for the development and calibration of control functions and advanced control has begun making inroads in several applications. However, there yet remains a predominance of manually tuned PID control algorithms and lookup tables often in the service of SISO control of subsystems. It is generally recognized that such control structures are expensive and complex to develop and tune[1] and inherently challenging to generalize into MIMO schemes or to accommodate changing constraints on actuators or engine states.

Model based techniques for control design, such as the model predictive control (MPC) approach discussed in this work, may be considered as a systematic approach to control development and calibration along with providing a multivariable control scheme that automatically accommodates actuator and state constraints. However, the implementation of MPC has remained elusive for several reasons. First, it is challenging to implement the run-time component within the limited footprint constraints of modern automotive electronic control units (ECUs). Second, a new control approach must consider the complex interactions with the associated functions within an ECU. Finally one must consider the needs of all of the developers and users who are required to interact with the control at each stage in the life cycle from functional development, software coding and testing, calibration, certification, and maintenance [18].

In Model Predictive Control (MPC) a model of the plant is used to *predict* the future evolution of the system [12]. Based on this prediction, at each time step t a performance index is optimized under operating constraints with respect to a sequence of future input moves in order to best follow a given trajectory. The first of such optimal moves is the *control* action applied to the plant at time t. At time $t+1$, a new optimization is solved over a shifted prediction horizon.

Parallel advances in theory and computing systems have enlarged the range of applications where real-time MPC can be applied [5], [10], [27]. Yet, for a wide class of "fast" applications the computational burden of nonlinear MPC is still a serious barrier for its implementation.

Nevertheless, the capability of handling constraints in a systematic way makes MPC a very attractive control technique, especially for applications where the process is required to work *in wide operating regions* and close to the boundary of the set of admissible states and inputs. In particular, a control strategy must consider the hierarchical architecture of typical automotive controllers and a subcontroller can be expected to accept and respond to time varying setpoints and constraints that are determined and distributed by a supervisory layer of functionality.

This paper describes several aspects of our work in developing control approaches for diesel engine air induction systems and discusses a subset of the relevant requirements to be met by the proposed control scheme. In particular we concentrate on the performance requirements of these controllers with respect to the highly nonlinear plants, and the requirements for retrofitting a new strategy into existing ECU architectures as a replacement for lower level control components.

The paper is structured as follows. Section II-A overviews the requirements imposed by real-world ECU considerations. Section II-B briefly discusses the physical characteristics of a representative example turbodiesel air induction system and includes a brief survey of prior work in modeling single-stage turbocharged systems with high-pressure exhaust gas recirculation (EGR). Section III presents our proposed explicit model predictive control approach including its parametriza-

Greg Stewart is with Honeywell, E-mail: greg.stewart@honeywell.com. Francesco Borrelli is with the University of California, Berkeley, E-mail: fborrelli@me.berkeley.edu

[1]This cost may be measured in terms of the engineering and test cell time required to develop and tune a controller.

978-1-4244-3124-3/08/$25.00 ©2008 IEEE

tion in terms of constraints. Section IV describes the implementation of the proposed control strategy on a 2.2 litre turbodiesel engine.

II. Problem Definition

A. Controller Implementation Environment

A controller designed for practical use in automotive applications must consider the restrictive computing environment into which it will be implemented. Depending on the application, current industrial ECUs may be expected to have a processor speed less than 60MHz and less than 3MB of flash memory. The loop time of a controller function depends on its purpose and the sample time of industrial air and EGR handling controllers is typically faster than 100ms. One must also consider that a single ECU will typically run several functions in addition to any function under development. This means that the implementation footprint of any developed function must be kept as small as possible when developing any new control function. The development of control functions should not only consider their coupling through the sharing of limited resources but also their functional interaction.

In current industrial practice a common approach to control architecture is to organize the control functionality in a hierarchical structure as illustrated in Figure 1 (see for example [18]). A supervisory function will determine the state of the engine system, which then distributes information to the individual subsystem controllers in the form of setpoints, feedforward actuator values, actuator constraints, and engine state constraints. Some standard components of the engine state include but are not limited to the engine speed, the quantity of fuel injected, ambient environmental conditions (such as pressure and temperature), turbocharger speed limitations, and special modes such as cold start and regeneration of an aftertreatment device. These signals are generally a function of the operation and ambient environment of the engine and necessarily change as a function of time. The time and effort required for the calibration of the subcontrollers to accommodate such time varying commands is considered to be a critical problem to practitioners (see [6] for example).

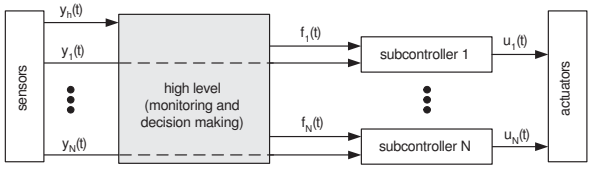

Fig. 1. A common architecture of automotive controller code. The symbols $y_i(t)$ and $u_j(t)$ represent the i^{th} and j^{th} subsets of sensor and actuator information respectively. The symbols $f_k(t)$ denote the information transferred to the k^{th} subcontroller and may include setpoints, feedforward actuator values, and time varying constraints for actuators and engine states. The MPC proposed in this article will replace one (or more) of the illustrated subcontrollers.

The requirements imposed by these considerations lead us to propose the model predictive control formulation described in Section III where we will present an MPC parameterized in terms of time varying constraints on inputs and outputs. In order to match the requirements imposed by practical calibration problems, the proposed approach permits the scheduling of the constraints as an arbitrary exogenous signal to the subcontrollers. This has the benefit of facilitating the retrofit of the proposed MPC approach into existing industrial ECUs. The application of MPC to turbodiesel problems has previously been considered in [8], [15]. In [15] the authors switch between explicit linear MPC controllers each valid for a certain range of operating points (engine speed and fuel rate). In [8] a full nonlinear MPC (NMPC) is proposed which demonstrates improved performance with respect to linear state feedback and input-output linearization approaches. As pointed out in [8], the main drawback of most NMPC techniques comes from the fact that they typically require far more computational power than is available on modern automotive ECUs.

B. Physical Plant and Closed-Loop Requirements

In this section we will overview the issues we have encountered when modeling the air induction system in turbocharged diesel engines that are the focus of our work. Turbodiesel engines present a rich variety of engine layouts and control problems. The turbocharger configurations may be single-stage or multiple-stage (parallel or series). The exhaust gas recirculation (EGR) may be implemented in a high pressure, low pressure, or blended EGR loop [23]. The turbocharger actuators may include bypass or wastegate valves and variable geometry turbines. Inroads are beginning to be seen in variable valve actuation (VVA).

The control goals of the air induction system are typically designed to achieve a balance between legislated emissions constraints (e.g. oxides of nitrogen (NOx) and particulate matter (PM)), drivability (torque response), and fuel economy considerations. The particular control configurations that are used to achieve these goals must take into account the sensors available for production engines. Common examples include intake manifold pressure (MAP), compressor flow sensors (MAF), manifold temperature sensors, EGR flow sensors, and turbospeed sensors. In addition, novel sensors which directly measure the emissions of the exhaust gases can be used for closed-loop control [20]. Closed-loop control of engine-out emissions is a promising method for ensuring that the aftertreatment devices receive an exhaust stream with a chemical composition appropriate for each flow rate and temperature.

The control oriented modeling for these systems may be approached systematically by integrating first-principles modeling with system identification techniques to create grey box models [7]. This process may be followed in order to derive models for various engine layout configurations that capture the essential input-output dynamics and nonlinearities required for the control of the system. As noted in [7], [9], [11], [15], [22], [26] (and references therein) models of air induction in diesel engines are highly nonlinear and the source of the nonlinearities may be attributed to the

dependencies of the various mass flow rates on the model states and exogenous inputs [22]. Let f and h denote the state update and output functions, respectively:

$$\dot{x}(t) = f(x, u, v), \qquad y(t) = h(x, u, v) \tag{1}$$

where y represent the controlled variables, the array u represents the actuator setpoints to be computed by the controller, and v represents the exogenous inputs to the system.

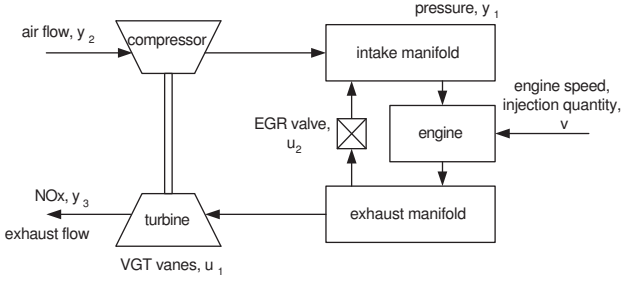

Fig. 2. Simplified engine layout of a single-stage turbocharged diesel engine with high pressure EGR.

A class of nonlinear systems (1) that has received considerable attention from the control community in recent years is that of a single-stage turbodiesel engine with high pressure EGR loop as illustrated in Figure 2. The controlled variables $y = [y_1, y_2]$ are intake manifold air pressure (MAP) and compressor flow (MAF) respectively and are controlled by $u = [u_1, u_2]$ being the variable geometry turbine (VGT) and EGR valve actuators respectively. The exogenous inputs $v = [v_1, v_2]$ are typically considered as the engine speed and the injected fuel quantity. Depending on the modeling requirements the exogenous variables may be extended to include additional parameters such as ambient conditions (temperature, pressure, moisture).

The nonlinearities of such a system can be particularly troublesome for control design. It was noted in [11], [22] that even the *sign* of the steady-state gain from the VGT actuator u_1 to the compressor flow y_2 may change when closing the VGT vanes, particularly when the high pressure EGR valve u_2 is in an open position. We have also found turbodiesel applications where the sign of the gain from u_1 to the intake manifold pressure y_1 changes as the VGT vanes are closed. Thus the consideration of these nonlinearities is crucial to the development of a practical controller. Engine data exhibiting both cases is illustrated in Figure 3.

Various authors use different formulations for the control oriented model of this system. In order to compare approaches, we will write down a linearized version of (1) as follows:

$$\begin{aligned} \dot{x}_\delta(t) &= A(\theta)x_\delta(t) + B(\theta)u_\delta(t) + E(\theta)v_\delta(t) \\ y_\delta(t) &= C(\theta)x_\delta(t) + D(\theta)u_\delta(t) + F(\theta)v_\delta(t) \end{aligned} \tag{2}$$

where $x_\delta(t) \in \mathbb{R}^n$, $u_\delta(t) \in \mathbb{R}^{n_u}$, $v_\delta(t) \in \mathbb{R}^{n_v}$, and $y_\delta(t) \in \mathbb{R}^{n_y}$, are the state, input, exogenous disturbance, and output

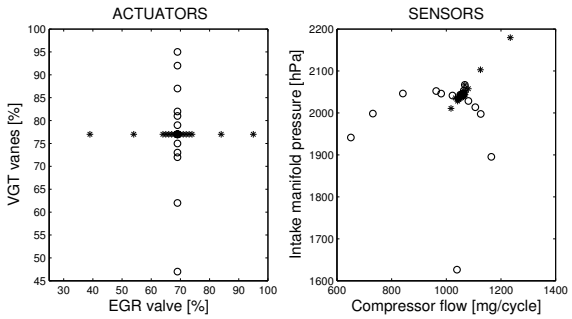

Fig. 3. Illustration of a steady-state nonlinearity observed experimentally at a fixed engine speed 2500rpm and fuelling rate 42.3 mm^3/cycle in the 2.2 litre turbodiesel engine used in Section IV. As the VGT vanes are closed, both the MAP and MAF initially increase, followed by a region where MAP increases and MAF decreases, ending in a region wherein both properties decrease with closing VGT vanes. (Compare with Figures 8 and 10 in [22]).

vector, respectively. The matrices A, B, C, D, E, F are continuous valued functions of $\theta : [0, \infty) \to \mathbb{R}^{n_\theta}$. Model (2) can be derived from a linearization of (1). In this case the signals in (2) must be interpreted as deviations from a parameter-dependant equilibrium $\{x_{eq}(\theta), u_{eq}(\theta), v_{eq}(\theta), y_{eq}(\theta)\}$ (also known as trim points) such that $x_\delta = x - x_{eq}(\theta)$, and the coefficient matrices are obtained from derivatives evaluated at the same equilibria such that $A(\theta) = \frac{\partial f}{\partial x}$ etc. Model (2) can also arise from an LPV or a quasi-LPV derivation then no equilibria points are required except for the origin and the signals in (2) are equivalent to the signals in (1) [17].

Typically the function θ is time varying and is a function of the exogenous variables v in (1). Depending on the modeling, θ may also be a function of the state variables x. For air induction in diesel engines the latter quasi-LPV case is discussed in [9], [26].

In [11] a nonlinear model (1) is used and the state vector $x \in \mathbb{R}^7$ is comprised of the pressures, densities, and fractions of inert gases for the intake and exhaust manifolds and the turbocharger rotational speed. This formulation is extended in [22] to include two additional states - one each to accommodate the dynamics of the VGT and EGR actuators. In the 3^{rd} order quasi-LPV models of [9] and [26], the states are given by intake manifold pressure, exhaust manifold pressure, and compressor power in the former case and by intake and exhaust manifold pressures and the compressor mass flow in the latter case. In [15] a linear dynamic model with $x \in \mathbb{R}^2$ is obtained from a black box identification experiment performed at each of 12 partitions of the engine speed and fuel plane[2].

In addition to the physical pressure and flow variables discussed above, the example in Section IV considers implementing a constraint on the (measured) engine-out NOx emissions. The control oriented modeling of engine-out emissions requires an additional understanding of the role of the properties of the inducted gas on the in-cylinder conditions that influence the formation of NOx. The interested

[2]Additional states are used in the controller design to represent engine speed, fuel quantity and offset errors.

reader is referred to [7], [21], [22], [24] for discussions and developments of NOx formation and modeling.

III. Explicit Model Predictive Controller

The following section describes the implementation of an explicit Model Predictive Controller (MPC) [1], [2]. We will first present the standard MPC scheme used. Then, we will enumerate a list of practical implementation issues which have been addressed by our research in order to implement the scheme on an industrial automotive ECU.

We consider a *piecewise affine* (PWA) discrete-time approximation of the system dynamics (1)

$$\begin{array}{rcl} x(k+1) & = & A_\sigma x(k) + B_\sigma u(k) + B^v_\sigma v(k) + f_\sigma \\ y(k) & = & C_\sigma x(k) + C^v_\sigma v(k) + g_\sigma \\ & & \text{for } \begin{bmatrix} x \\ u \\ v \end{bmatrix}(k) \in \mathcal{C}_\sigma \end{array} \quad (3)$$

where $x(k)$, $u(k)$, $y(k)$, $v(k)$, are the state, input, output and exogenous disturbances (either measured or estimated), respectively at time kT_s where T_s is the sampling time. The natural number $\sigma(k) \in \{1, 2, \ldots, M\}$ is the operating point at time kT_s and it is a function of inputs $u(k)$, states $x(k)$ and disturbances $v(k)$. The set $\{\mathcal{C}_\sigma\}_{i=1}^M$ is a polyhedral partition of the state, input and measured disturbance set. System (3) is subject to the following time varying constraint on inputs and outputs for all $k \geq 0$.

$$u(k) \in \mathcal{U}(u_{min}(k), u_{max}(k)),\ y(k) \in \mathcal{Y}(y_{min}(k), y_{max}(k)) \quad (4)$$

where $\mathcal{U}(k)$ and $\mathcal{Y}(k)$ are polyhedra for all $k \geq 0$.

Remark 1: We remark that there is a difference between the scheduling of a plant *model* in which the equilibrium points or parameters of an LPV model are scheduled as a function of θ in (2), and the scheduling of the *controller* with a function σ. It is quite common in practice that the controller scheduling $\sigma \neq \theta$, where the function σ may represent a simplification of a higher fidelity scheduling function θ.

To clarify further. The usual interpretation of θ is that a nonlinear system (1) is equivalent to (or approximated by) a linear system such as the parameterized model family in (2) for frozen values of the scheduling variable $\theta(t) = \theta_0$ [17]. In [15], [22], [25] the respective authors design the controller scheduling such that the controller gains are scheduled with σ as a function[3] of engine speed and injected fuel quantity. On the other hand Figure 3 above (and Figures 8 and 10 in [22]) illustrate that the plant remains highly nonlinear at fixed values of engine speed and fuel flow and thus $\sigma \neq \theta$ for the usual interpretation of θ. □

Consider the problem of letting the output of system (3) track a given reference $y_{ref,k}$ while satisfying input and output constraints (4). Assume that estimates/measurements of the state $x(k)$ and disturbances $v(k)$ are available at the current time k and consider the following cost function

$$\begin{array}{l} J_k(x, v, w, \Delta U, \epsilon) \triangleq \|y_{H_p+k|k} - y_{ref,H_p+k|k})\|_2^P + \\ \quad + \sum_{t=k}^{H_p-1} \|(y_{t|k} - y_{ref,t|k})\|_2^Q + \|\delta u_{t|k}\|_2^R + \rho\epsilon^2 \end{array} \quad (5)$$

where $\|v\|_2^M = v'Mv$. Then, the finite time optimal control problem is solved at time k,

$$\begin{array}{lll} \min\limits_{\Delta U_{H_c|k}, \epsilon} & J_k(x(k), v(k), w(k), \Delta U_{H_c|k}, \epsilon) & (6a) \\ \text{s.t.} & x_{k+1|k} = A_\sigma x_{k|k} + B_\sigma u_{k|k} + & \\ & \quad + B^v_\sigma v_{k|k} + B^w_\sigma w_{k|k} + f_\sigma & \\ & w_{k+1|k} = A^w_\sigma w_{k|k} + B^u_\sigma u_{k|k} & \\ & y_{k|k} = C_\sigma x_{k|k} + C^v_\sigma v_{k|k} + C^w_\sigma w_{k|k} + g_\sigma & (6b) \\ & \text{if } \begin{bmatrix} x \\ u \\ v \\ w \end{bmatrix}_{k|k} \in \mathcal{C}_\sigma & (6c) \\ & u_{t|k} = \delta u_{k|k} + u_{k-1|k} & \\ & u_{t|k} \in \mathcal{U}(u_{min}(k), u_{max}(k)), & (6d) \\ & y_{t|k} \in \mathcal{Y}(y_{min}(k), y_{max}(k)) \oplus \epsilon & (6e) \\ & \quad t = k, \ldots, k + H_c,\ \epsilon > 0 & \\ & \delta u_{t,k} = 0, \quad t = k + H_c, \ldots, k + H_p & (6f) \\ & v_{t|k} = v_{t-1|k}, \quad t = k + 1, \ldots, k + H_p & (6g) \\ & x_{k+H_p|k} \in \mathcal{X}_f & (6h) \\ & u_{k|k} = u(k-1) & (6i) \\ & x_{k|k} = x(k),\ w_{k|k} = w(k),\ v_{k|k} = v(k) & (6j) \end{array}$$

where the column vector $\Delta U_{H_c|k} \triangleq [\delta u'_{k|k}, \ldots, \delta u'_{H_c-1|k}]'$ and ϵ are the optimization vectors, H_p and H_c denote the output prediction horizon and the control horizon and $\mathcal{X}_f$ is the terminal region.

Let $\Delta U^*_{H_c|k} = \{\delta u^*_{k|k}, \ldots, \delta u^*_{k+H_c-1|k}\}$ and ϵ^* be the optimal solution of (5)-(6) at time k. Then, the first sample of $U^*_{H_c|k}$ (obtained from $\Delta U^*_{H_c|k}$ and $u(k-1)$) is applied to the system:

$$u(k) = u^*_{k|k}. \quad (7)$$

The optimization (5)-(6) is repeated at time $k+1$, based on the new state $x_{k+1|k+1} = x(k+1)$, exogenous disturbances $v_{k+1|k+1} = v(k+1)$, additive disturbances $w_{k+1|k+1} = w(k+1)$, input and output constraints, yielding a *moving* or *receding horizon* control strategy.

In (5) we assume that $Q = Q' \succeq 0$, $R = R' \succ 0$, $P \succeq 0$.

Remark 2: Compared to the original model (3), the model (6b) used in the MPC is augmented with an additional state $w(k) \in \mathbb{R}^{n_w}$. The vector $w(k)$ is an additive disturbance which is used to model the mismatch between the nonlinear system (1) and its PWA model (3) [13]. □

In problem (5)-(6) the following assumptions are used

- A1 $H_p > H_c$ and the control signal is assumed constant for all $H_c \leq k \leq H_p$. This allows the reduction of the computational complexity of the MPC scheme.
- A2 The exogenous disturbance v is assumed constant over the horizon. If PWA prediction models for $v(k)$ are available they could be include in the MPC formulation (5)-(6).

[3] In [22], [25] the controller scheduling function $\sigma : \mathcal{R}^2 \to \mathcal{R}^{n_\theta}$ is continuous, while in [15] it has the form $\sigma : \mathcal{R}^2 \to \mathcal{N}$ and serves the purpose of deciding between one of 12 linear MPC controllers.

A3 Constant region σ over the horizon (6c).

A4 Soft Constraints on outputs, i.e. $\mathcal{Y}(y_{min}(k), y_{max}(k)) \oplus \epsilon \triangleq \{y | y + \epsilon \in \mathcal{Y}(y_{min}(k), y_{max}(k))\}$.

Remark 3: Assumption (A3) basically implies that for any given time *we simply implement a linear MPC for one member of the set of linear systems*. Ideally the assumption should be removed in order to predict switches between affine dynamics over the horizon H_p. This would improve both performance and attractivity region of the closed loop system. Nevertheless, we have been forced to use assumption (A3) by the current limitations of automotive ECU. In fact, by removing (A3), problem (5)-(6) becomes a mixed integer quadratic program (MIQP) whose explicit solution [2] requires more floating point operations for its evaluations and more memory for its storage. □

The optimization problem (5)-(6) can be recast as a quadratic program (QP) .

$$\begin{aligned} \min_{\Delta U_{H_c|k}, \epsilon} \quad & \tfrac{1}{2}\Delta U_{H_c|k}{}' H \Delta U_{H_c|k} + H_\epsilon \epsilon^2 + \\ & + \phi(k)' F \Delta U_{H_c|k} \\ \text{subj. to} \quad & G\Delta U_{H_c|k} \leq W + E\phi(k) \end{aligned} \tag{8}$$

where $\phi(k) \triangleq [x\ u(k-1)\ v(k)\ w(k)\ u_{min}\ u_{max}\ y_{min}\ y_{max}]$ and $\phi(k) \in \mathbb{R}^{n_p}$. Problem (8) is a multiparametric quadratic program that can be solved by using the algorithm presented in [1]. Once the multiparametric problem (8) has been solved, the solution $\Delta U^*_{H_c|k} = \Delta U^*_{H_c|k}(\phi(k))$ of problem (5)-(6) and therefore $u^*(k) = u^*(x(k))$ is available explicitly as a function of the set of parameters $\phi(k)$ for all $\phi(k) \in \mathcal{X}_0$. $\mathcal{X}_0 \subseteq \mathbb{R}^{n_p}$ is the set of initial parameters $\phi(0)$ for which the optimal control problem (5)-(6) is feasible. The following result [1] establishes the analytical properties of the optimal control law and of the value function.

Theorem 1: [1] The control law $\delta u^*(k) = f_\sigma(\phi(k))$, $f_\sigma : \mathbb{R}^{n_p} \to \mathbb{R}^m$, obtained as a solution of (8) is continuous and piecewise affine on polyhedra

$$f_\sigma(\phi) = F^i_\sigma \phi + g^i_\sigma \quad \text{if} \quad \phi \in CR^i_\sigma, \quad i = 1, \ldots, N^r_\sigma \tag{9}$$

where the polyhedral sets $CR^i_\sigma = \{\phi \in \mathbb{R}^{n_p} | H^i_\sigma \phi \leq K^i_\sigma\}$, $i = 1, \ldots, N^r$ are a partition of the feasible polyhedron $\mathcal{X}_0$.

As discussed in [1] the implicit form (8) and the explicit form (9) are *equal*, and therefore the stability, feasibility, and performance properties are automatically inherited by the piecewise affine control law (9). Clearly, the explicit form (9) has the advantage of being easier to implement, M lookup tables, one for each operating point σ, are uploaded on the ECU and at each time step k the MPC resorts to selecting the current operating point σ, searching for the region CR^j_σ containing the current vectors of parameters $\phi(k)$ and implementing the corresponding controller $F^j_\sigma \phi(k) + g^j_\sigma$.

The following lists some of the major practical issues which have been encountered while implementing the proposed MPC on an automotive ECU. In this paper we will focus on only the final listed issue.

- State estimation. Estimation of the state $x(k)$ and $w(k)$ of system (3) is a nontrivial task. We have used a bench of M Kalman filters which run in parallel in order to smoothen the estimation during switch between different operating points.
- No offset. In order to obtain offset-free control with MPC, the PWA system model (3) is augmented with a constant disturbance model (included in $w(k)$ in system (6c)) which is used to estimate and predict a constant mismatch between measured and predicted outputs. The state and disturbance estimates are used to initialize the MPC problem [4], [16].
- Limited ECU memory. We had to modify the explicit implementation in order to be able to run the MPC (5)-(7) in an industrial ECU (even for short horizons). We have used the Karush-Kuhn-Tucker conditions which lead to (9) in order to reduce the memory required for storing F_σ and g_σ in (9). More details can be found in [3].
- Time-varying actuator and state constraints. In contrast to techniques such as [15], the proposed formulation has been designed to address constraints that vary arbitrarily as a function of time and thus independently of the state variables or gain scheduling parameters.
- Constraint satisfaction under steady state disturbances. For a range of steady-state exogenous disturbance $v(k) = \bar{v}$ the reference y_{ref} might be infeasible for the given input and output constraints and thus not be trackable. At steady-state, the objective function will be composed of two terms with conflicting objectives: satisfy the constraints ($\rho\epsilon^2$) and track y_{ref}. In addition, model uncertainty and high ρ weights (usually used to strictly enforce soft constraints) can lead to oscillating behavior and poor performance (see Section IV for experimental evidence). We solved this problem as follows. For each operating point σ we compute a feasible polyhedron $\mathcal{F}_\sigma$ in the space of the variables y_{ref}, $\bar{v}$, $\bar{w}$, u_{min}, u_{max}, y_{min}, y_{max}, where y_{ref}, $\bar{v}$ and $\bar{w}$ are references, exogenous disturbances and additive disturbances at steady state, respectively. If at time instant k the vector $[y_{ref}\ \bar{v}\ \bar{w}\ u_{min}\ u_{max}\ y_{min}\ y_{max}]$ belongs to $\mathcal{F}_{\sigma(k)}$, then the reference y_{ref} is feasible and no action is taken. If the vector $[y_{ref}\ \bar{v}\ \bar{w}\ u_{min}\ u_{max}\ y_{min}\ y_{max}]$ does not belong to $\mathcal{F}_{\sigma(k)}$ then y_{ref} is not feasible and the weights in the cost function (5) are modified by bringing Q to zero and increasing ρ. In this way, the controller will try to satisfy the constraints and do not try the tracking of the infeasible outputs. Below we show how to compute $\mathcal{F}_\sigma$ in the case A_σ has no eigenvalues at 1. We remark that this approach is similar but less computationally expensive than the one used to compute feasible references at each time step in [16].

From model (6b) we write

$$y_{k|k} = C_\sigma x_{k|k} + C^v_\sigma v_{k|k} + C^w_\sigma w_{k|k} + g_\sigma$$

By using model (6b) and considering all values at steady state (denoted by a barred symbol), we can write

$$\bar{x} = (I - A_\sigma)^{-1} [B_\sigma \bar{u} + B^v_\sigma \bar{v} + B^w_\sigma \bar{w} + f_\sigma]$$

and thus

$$\bar{y} = C_\sigma (I - A_\sigma)^{-1} [B_\sigma \bar{u} + B_\sigma^v \bar{v} + B_\sigma^w \bar{w} + f_\sigma + C_\sigma^v \bar{v} + C_\sigma^w \bar{w} + g_\sigma] \quad (10)$$

We project the set described by (10) and by the constraint sets

$$\bar{u} \in \mathcal{U}(u_{min}(k), u_{max}(k)),$$
$$\bar{y} \in \mathcal{Y}(y_{min}(k), y_{max}(k))$$

into the space $[\bar{y}\ \bar{v}\ \bar{w}\ u_{min}\ u_{max}\ y_{min}\ y_{max}]$ and then set $\bar{y} = y_{ref}$. The result is a polyhedron $\mathcal{F}_\sigma$ which identifies if the reference y_{ref} is feasible for a fixed $[\bar{v}\ \bar{w}\ u_{min}\ u_{max}\ y_{min}\ y_{max}]$ and a fixed operating point σ.

IV. Presentation and Discussion of Results

Section III has proposed an MPC framework and gave an overview of some major technical obstacles that were overcome in the course of its development in order to satisfy the requirements of Section II. Given the limitations of space, in this Section we provide an on-engine example where we concentrate on the issue of time-varying constraint satisfaction under steady-state disturbance discussed above.

The engine was a 2.2 litre, Euro IV certified, turbocharged diesel engine with a variable geometry turbine and a high pressure EGR loop as illustrated in Figure 2. The ECU bypass was executed using an "on-target" rapid prototyping system (*ATI No-Hooks OnTarget* [14]) in which the designed controllers were downloaded into a common industrial ECU - a Motorola MPC555 - with a 40MHz processor and 2MB flash memory.

The control variables in question are the intake manifold pressure (y_1), the compressor air flow (y_2). We will consider imposing constraints on the engine-out NOx emissions (y_3). Active control over engine-out NOx has potential application in forming a part of a coordinated engine and NOx aftertreatment control strategy. The actuators are the VGT vane position (u_1) and the EGR valve position (u_2). In this example we will concentrate on the operating point defined by fixed values of the exogenous inputs fuel injection quantity of 42.3mm^3/cycle and an engine speed of 2500rpm, actuator positions of 77% (0=open, 100=closed) for the VGT vanes and 69% (0=closed, 100=open) for the EGR valve corresponding to an intake manifold pressure of 207kPa, a compressor flow of 1119mg/cycle and engine-out NOx emissions of 379ppm. The production inline NOx sensor was located downstream of the turbine. The sample time of the control was 100ms.

Referring to the piecewise affine model in (3) and considering the fuel quantity (v) as a measured exogenous disturbance of the local linear model, we can write down a linear dynamic model of the plant at this operating point as

$$\begin{bmatrix} y_1 \\ y_2 \\ y_3 \end{bmatrix} = \begin{bmatrix} g_{11}(q) & g_{12}(q) \\ g_{21}(q) & g_{22}(q) \\ g_{31}(q) & g_{32}(q) \end{bmatrix} \begin{bmatrix} u_1 \\ u_2 \end{bmatrix} + \begin{bmatrix} g_{13}(q) \\ g_{23}(q) \\ g_{33}(q) \end{bmatrix} v \quad (11)$$

As discussed in Section II-B above, grey-box models of the turbodiesel engine elements found in the literature may be up to 7^{th} order. In this case, engine in question was found to be well-modeled using first order transfer functions for each of the elements $g_{ij}(q)$,

$$g_{ij}(q) = \frac{b_{ij} q^{-1}}{1 - a_{ij} q^{-1}} \quad (12)$$

the numerical values of the coefficients a_{ij}, b_{ij} that resulted from a black-box model identification may be found in the Appendix.

To illustrate the proposed approach we will consider the practically-motivated problem of a designer who wishes to implement tracking of intake manifold pressure y_1 and compressor flow y_2 in (11) to exogenous setpoint targets $y_{1,ref}$ and $y_{2,ref}$ while respecting exogenous constraints as described in (4) and (6)

$$u_{min}(k) = \begin{bmatrix} 5 \\ 5 \end{bmatrix}, \quad u_{max}(k) = \begin{bmatrix} 95 \\ 95 \end{bmatrix}, \quad (13)$$

$$y_{3,max}(k) = \overline{\mathrm{NOx}}(k) \quad (14)$$

for all k where $\overline{\mathrm{NOx}}(k)$ are time-varying max NOx constraints and all the other outputs are unconstrained. As discussed in Section II-A, $\overline{\mathrm{NOx}}(k)$ in (14) could be imposed on a low level subcontroller by a higher level function in the control hierarchy. The identified models and constraints in (11)–(14) were next used in a MPC problem of the form (6) with no terminal constraint and with $H_c = 1$, $H_p = 40$, $Q = 0.25 \cdot I_2$, and $R = 128 \cdot I_2$ in (5). The attractivity region of the nominal closed-loop system can be calculated by using reachable set algorithms for PWA systems [2]. Robustness to parameter uncertainty has been validated by extensive experimental testing. The closed-loop results in Figures 4-6 were obtained using a soft constraint parameter $\rho = 10^6$ in (6).

Figure 4 illustrates the performance of the controller as it simultaneously tracks changing setpoints in MAP and MAF y_1 and y_2 respectively. The constraint on the engine-out NOx y_3 was set to a very high value of $\overline{\mathrm{NOx}}(k) =$ 2000ppm in order to demonstrate the unconstrained closed-loop performance. Next the NOx constraint was lowered to $\overline{\mathrm{NOx}}(k) =$ 410ppm and the ability of the controller to accommodate this tightened constraint is illustrated in Figure 5 when subject to the same setpoint steps as Figure 4. However, when the NOx constraint is further lowered to $\overline{\mathrm{NOx}}(k) =$ 390ppm we observe the closed-loop instability illustrated in Figure 6.

The reason for this instability may be understood by considering the effect of the soft constraint parameter ρ in (6) and the degree to which the output constraint has been violated. A large value for ρ and a larger degree of constraint violation result in the MPC problem generating a very aggressive control action in an effort to return to a feasible position. The combination of such an aggressive controller along with the inevitable model uncertainty associated with with real systems leads to the instability illustrated in Figure 6.

The controller is then retuned with a smaller value of $\rho = 10^3$ in (6). As illustrated in Figure 7, using a less

aggressive value of ρ allows the closed-loop to satisfy the tighter constraint on NOx emissions $\overline{\text{NOx}}(k) = 390$ppm in (14).

The examples illustrated in Figures 4-7 were selected in order to highlight the delicate interaction between the soft constraint parameter ρ and the output constraints and to motivate the development described in Section III in which the tuning of the controller is switched as a function whether or not the reference y_{ref} is evaluated to be feasible or unfeasible. In fact, experimental results have shown that detuning is very complex when the controller has to operate in wide operating regions subject to larger uncertainties.

The current implementation includes the switched tuning proposed in Section III and several operating points which cover the whole operating region of the engine. The results on the transient FTP cycle will be included in a manuscript which is under preparation.

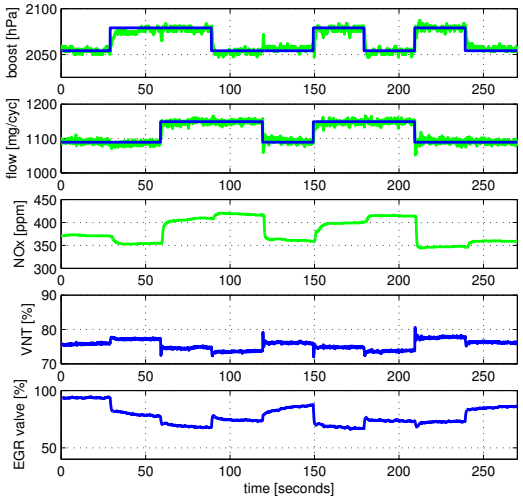

Fig. 4. Closed-loop run showing response to setpoint y_{ref} changes in y_1 (manifold air pressure) and y_2 (compressor flow) with controller tuning $N = 1$, $Ny = 40$, $Q = 0.25 \cdot I_2$, and $R = 128 \cdot I_2$ in (5). The constraint on NOx (y_3)was set to $\overline{NOx}(k) = 2000$ppm in (14) to illustrate the unconstrained closed-loop performance.

V. Conclusions

In this article we have discussed several requirements for the practical control of industrial diesel powertrains. These included the computational requirements imposed by the limited computing resources, the hierarchical architecture of existing software, and time-varying constraints. In addition the requirements imposed by the highly nonlinear air induction problems under consideration must be addressed in any successful control design. This article proposed an explicit model predictive control (MPC) approach designed to work with the time-varying setpoints and constraints as are required from the low-level control layer in the hierarchy.

The proposed approach was demonstrated on production ECU controlling a real 2.2 litre diesel engine in which the

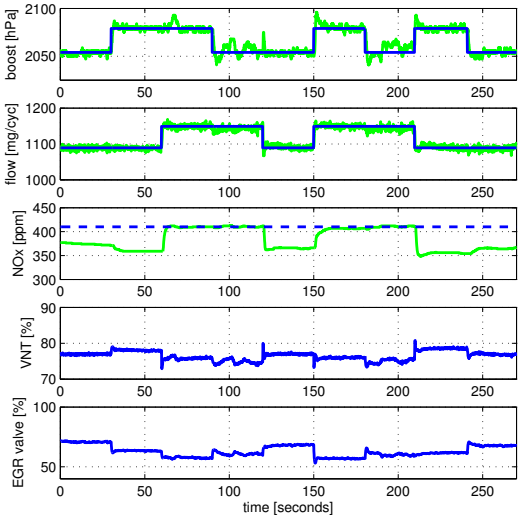

Fig. 5. The constraint on NOx emissions is stepped down to $\overline{NOx}(k) = 410$ppm in (14) with an aggressive soft constraint parameter of $\rho = 10^6$ in (6).

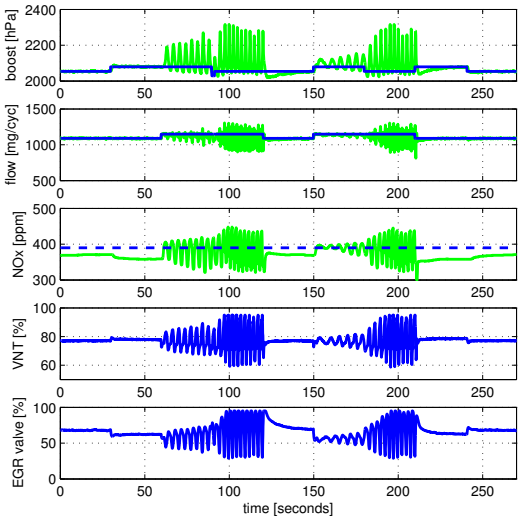

Fig. 6. The constraint on NOx is further reduced to $\overline{NOx}(k) = 390$ppm in (14) for the same controller used in Figures 4 and 5. The combination of an aggressive soft constraint parameter and a higher degree of constraint violation led to a overly-active controller resulting in the illustrated closed-loop instability. (Note that the y-axis has a different scale relative to Figures 4, 5, and 7.)

VGT and EGR actuators were used to track setpoints on MAP and MAF while respecting a time-varying constraint on engine-out NOx emissions. The example underscores the nature of interaction between output constraints and model uncertainty.

References

[1] A. Bemporad, M. Morari, V. Dua, and E.N. Pistikopoulos. The explicit linear quadratic regulator for constrained systems. *Automatica*,

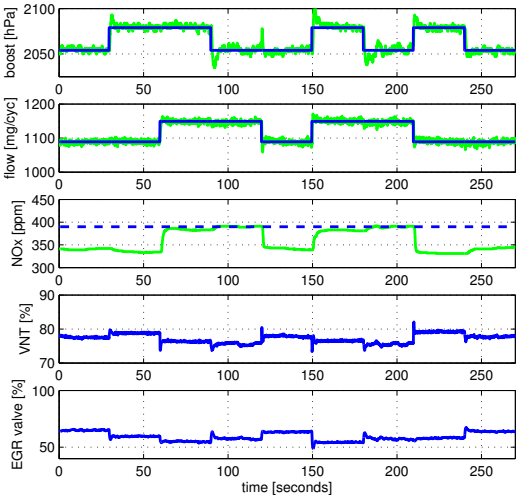

Fig. 7. Controller tuning same as Figures 5-6 but with a reduced value of the soft constraint parameter $\rho = 10^3$ in (6). In contrast to Figure 6 it may be observed that the more conservative approach to output constraints achieves a stable closed-loop while satisfying the constraint $\overline{NOx}(k) =$ 390ppm in (14).

38(1):3–20, 2002.

[2] F. Borrelli. *Constrained Optimal Control of Linear and Hybrid Systems*, volume 290 of *Lecture Notes in Control and Information Sciences*. Springer, 2003.

[3] F. Borrelli, M. Baotic, J. Pekar, and G. Stewart. On the Complexity of Explicit MPC Algorithms. Technical Report. http://www.me.berkeley.edu/∼frborrel/pub.php, August 2008.

[4] F. Borrelli and M. Morari. Offset free model predictive control. In *Proc. 46th IEEE Conf. on Decision and Control*, pages 1245–1250, 2007.

[5] H. J. Ferrau, H. G. Bock, and Moritz Diehl. An online active set strategy for fast parametric quadtratic programming in mpc applications. *IFAC Workshop on Nonlinear Model Predictive Control for Fast Systems, plenary talk*, 2006.

[6] L. Guzzella and A. Amstutz. Control of diesel engines. *IEEE Control Systems Magazine*, 18(2):53–71, 1998.

[7] L. Guzzella and C.H. Onder. *Introduction to Modeling and Control of Internal Combustion Engines*. Springer-Verlag, Berlin Heidelberg, 2004.

[8] M. Herceg, T. Raff, R. Findeisen, and F. Allgower. Nonlinear model predictive control of a turbocharged diesel engine. In *Proceedings of 2006 IEEE Conference on Control Applications*, pages 2766–2771, 2006.

[9] M. Jung and K. Glover. Control-oriented linear parameter-varying modelling of a turbocharged diesel engine. In *Proceedings of 2003 IEEE Conference on Control Applications*, pages 155–160, 2003.

[10] T. Keviczky and G. J. Balas. Flight test of a receding horizon controller for autonomous uav guidance. In *Proc. American Contr. Conf.*, 2005.

[11] I.V. Kolmanovsky, A.G. Stefanopoulou, P.E. Moraal, and M. van Nieuwstadt. Issues in modeling and control of intake flow in variable geometry turbocharged engines. In *18th IFIP Conference on System Modelling and Optimization*, 1997.

[12] D.Q. Mayne, J.B. Rawlings, C.V. Rao, and P.O.M. Scokaert. Constrained model predictive control: Stability and optimality. *Automatica*, 36(6):789–814, June 2000.

[13] K. R. Muske and T. A. Badgwell. Disturbance modeling for offset-free linear model predictive control. *Journal of Process Control*, 12:617–632, 2002.

[14] ATI No-Hooks OnTarget. www.accuratetechnologies.com. 2008.

[15] P. Ortner and L. del Re. Predictive control of a diesel engine air path. *IEEE Transactions on Control Systems Technology*, 15(3):449–456, May 2007.

[16] G. Pannocchia and J. B. Rawlings. Disturbance models for offset-free model predictive control. *AIChE Journal*, 49(2):426–437, 2003.

[17] W.J. Rugh and J.S. Shamma. Research on gain scheduling. *Automatica*, pages 1401–1425, September 2000.

[18] J. Schauffele and T. Zurawka. *Automotive Software Engineering: Principles, Processes, Methods, and Tools*. SAE International, Warrendale, PA, 2005.

[19] C.M. Schär. *Control of a Selective Catalytic Reduction Process*. PhD thesis, Diss. ETH Nr. 15221, Measurement and Control Laboratory, ETH Zurich, Switzerland, 2003.

[20] A. Schilling, E. Alfierir, A. Amstutz, and L. Guzzella. Emissions-controlled diesel engines. *MTZ - Motortechnische Zeitschrift*, 68(11):27–31, 2007.

[21] A. Schilling, A. Amstutz, C.H. Onder, and L. Guzzella. A real-time model for the prediction of the NOx emissions in DI diesel engines. In *Proceedings of 2006 IEEE Conference on Control Applications*, pages 2042–2047, 2006.

[22] A.G. Stefanopoulou, I. Kolmanovsky, and J.S. Freudenberg. Control of variable geometry turbocharged diesel engines for reduced emissions. *IEEE Trans. Contr. Syst. Technol.*, 8(4):733–745, July 2000.

[23] M. van Aken, F. Willems, and D-J de Jong. Appliance of high EGR rates with a short and long route EGR system on a heavy duty diesel engine. *SAE Technical Paper Series*, 2007-01-0906, 2007.

[24] R. van Helden, R. Verbeek, F. Willems, and R. van der Welle. Optimization of urea SCR deNOx systems for HD diesel applications. *SAE Technical Paper Series*, 2004-01-0154, 2004.

[25] M.J. van Nieuwstadt, I.V. Kolmanovsky, P.E. Moraal, A. Stefanopoulou, and M. Jankovic. EGR-VGT control schemes: Experimental comparison for a high-speed diesel engine. *IEEE Control Systems Magazine*, 20(3):63–79, June 2000.

[26] X. Wei and L. del Re. Gain scheduled H-infinity control for air path systems of diesel engines using LPV techniques. *IEEE Transactions on Control Systems Technology*, 15(3):406–415, May 2007.

[27] V. M. Zavala, C. D. Laird, and L. T. Biegler. Fast solvers and rigorous models: Can both be accomodated in nmpc? *IFAC Workshop on Nonlinear Model Predictive Control for Fast Systems, plenary talk*, 2006.

APPENDIX

The coefficients a_{ij} and b_{ij} in the dynamical model of the engine in (11) and (12) are given by,

$$\begin{bmatrix} a_{11} & a_{12} & a_{13} \\ a_{21} & a_{22} & a_{23} \\ a_{31} & a_{32} & a_{33} \end{bmatrix} = \begin{bmatrix} 0.9756 & 0.9244 & 0.9367 \\ 0.9582 & 0.9095 & 0.9342 \\ 0.9639 & 0.9658 & 0.9768 \end{bmatrix},$$

$$\begin{bmatrix} b_{11} & b_{12} & b_{13} \\ b_{21} & b_{22} & b_{23} \\ b_{31} & b_{32} & b_{33} \end{bmatrix} = \begin{bmatrix} 0.1235 & -0.1446 & 1.783 \\ -0.632 & -0.2427 & 1.111 \\ -0.558 & -0.02537 & 0.147 \end{bmatrix}$$